

HEXTE STUDIES OF SCO X-1 SPECTRA: DETECTIONS OF HARD X-RAY TAILS BEYOND 200 keV

F. D'Amico^{1, 2}, W. A. Heindl¹, R. E. Rothschild¹, L. E. Peterson¹,
D. E. Gruber¹, M. Pelling¹, and J. A. Tomsick¹

¹UCSD/CASS, 9500 Gilman Dr., La Jolla, CA 92093-0424, USA

²INPE, Av. dos Astronautas 1758, 12227-010 S. J. dos Campos - SP, Brazil

ABSTRACT

Using the HEXTE experiment on-board the *RXTE* satellite, we performed a search for hard X-ray tails in Sco X-1 spectra. We found strong evidence for the presence of such a non-thermal component on several occasions. Using the PCA/*RXTE* we were able to track the position of the source along the Z diagram, and we observed that the presence of the hard X-ray tail is not confined to a particular region. However, we found a correlation between the power law index of the non-thermal component and the position of the source in the Z diagram, suggesting that the hard X-ray spectrum (i.e., $E > 50$ keV) becomes flatter as the mass accretion rate increases. We were also able to study the temporal variation of the appearance/absence of the hard X-ray component. With our derived luminosities, we were also able to test the idea that X-ray luminosities can be used to distinguish between X-ray binary systems containing neutron stars and black holes.

INTRODUCTION

It is well established, after the *GRANAT*/SIGMA and *CGRO* missions, that a power-law spectra extending beyond 30 keV are not exclusive signatures of a black hole in an X-ray binary system (Barret and Vedrenne, 1994; Barret, McClintock, and Grindlay, 1996). High sensitivity observations with *RXTE* (e.g., Heindl and Smith, 1998; Barret et al., 2000) have shown the presence of hard X-ray flux in other types of low-mass X-ray binaries (LMXBs) and *BeppeSAX* observations also have detected hard X-ray flux from LMXBs systems (see, e.g., Frontera et al., 2000; Iaria et al., 2000; Di Salvo et al., 2000).

In this work we studied the hard X-ray spectrum of Sco X-1, a high luminosity LMXB Z source, using the High Energy X-ray Timing Experiment (HEXTE) on-board *RXTE*. The presence of a non-thermal component in Sco X-1 spectra has been historically reported (e.g., Peterson and Jacobson, 1966; Haymes et al., 1972; Duldig et al., 1983), but much more sensitive searches have failed to detect such a component, placing strong upper limits on the non-thermal flux (e.g., Greenhill et al. 1979; Rothschild et al., 1980; Soong and Rothschild, 1983). Recently, Strickman and Barret (2000) reported the presence of a hard X-ray tail in Sco X-1 using *CGRO*/OSSE. Thanks to the HEXTE sensitivity, we show here, on several occasions, strong evidence for the presence of this variable non-thermal component extending up to 220 keV.

This present study is an extension of a previous work (D'Amico et al., 2000) with the use of an expanded database from the public *RXTE* archive of Sco X-1 observations, containing data from 1997 April to 1999 July. Our on-source time (for the Proportional Counter Array, PCA) is 203,440 s in 22 subsets of data (an improvement factor of 30 % over our previous study) which, in turn, provided us with more than 100 ks of on-source live time in HEXTE. In the next sections we describe our data selection and analysis, then we discuss the detection of a non-thermal component and present our conclusions.

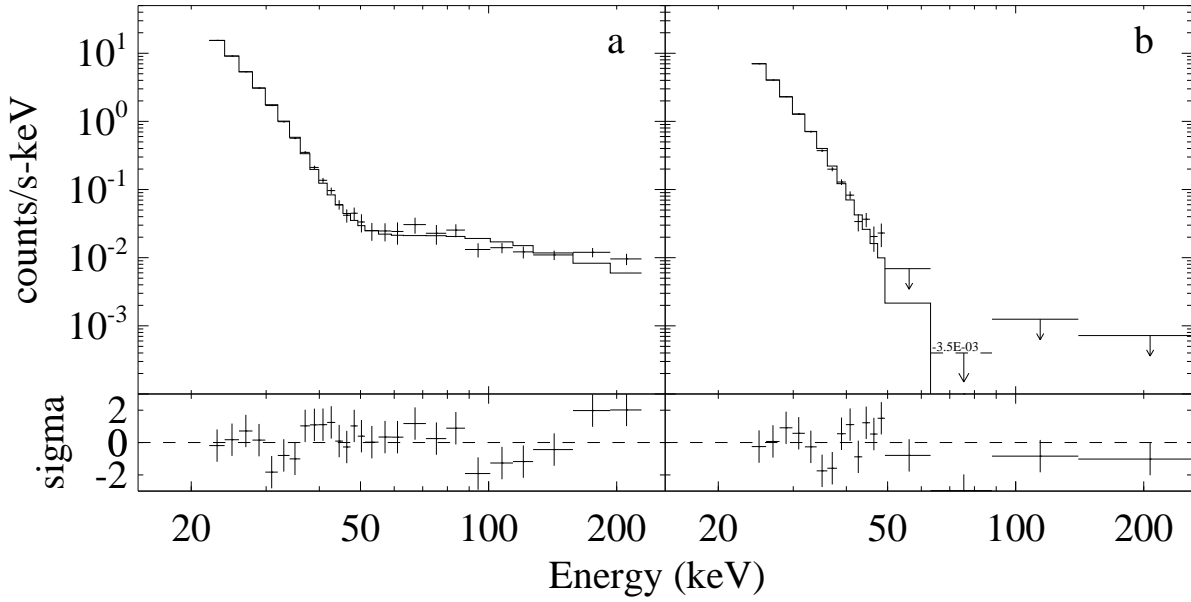


Fig. 1. Spectrum resulting from a bremsstrahlung + power law fit to data subset 20053-01-02-00 (a), and the result of a bremsstrahlung fit to subset 30035-01-04-00 (b), showing the presence/absence of a hard X-ray tail in Sco X-1. Residuals are given in units of standard deviations (lower panels). In (b) the upper limits are 2σ including the 60–80 keV bin which experienced a -3σ residual. The χ^2_ν are 1.27 and 1.62 respectively.

DATA SELECTION AND ANALYSIS

We used data from HEXTE (Rothschild et al., 1998) to search for hard X-ray tails in Sco X-1 in the ~ 20 – 220 keV interval and data from PCA (Jahoda et al., 1996) to determine the position of the source in the Z diagram. We have chosen, from the public *RXTE* database of Sco X-1, those subsets of data in which $\gtrsim 5000$ s of HEXTE total on-source time was available, in order to achieve good sensitivity at high energies, resulting in 22 *RXTE* observations (as of 2000 August) that cover the period from 1997 April to 1999 July. If, in a particular observation, the source was moving back and forth from the normal to the flaring branch (see, e.g., van der Klis, 1995), then we split the data according to the branch resulting in the 28 observation segments displayed in Table 1. Since we are primarily interested in the study of the non-thermal ($\gtrsim 50$ keV) spectra of the source (the “hard” component of the spectrum), we have simply modeled the (HEXTE) low energy thermal component as thermal bremsstrahlung emission.

We refer the reader to D’Amico et al. (2000), for a more detailed description of the instrument and data analysis.

RESULTS

We developed two criteria to determine the presence of a hard X-ray tail in a particular spectrum: 1) a signal to noise ratio (SNR) ≥ 5 in the 75–220 keV energy range, and 2) an F-Test null significance for the addition of the hard component at a level of 10^{-7} or less. We claim that we observed a hard X-ray tail **only** when both of these criteria are fulfilled. We have 8 clear detections of non-thermal flux in Sco X-1 spectra, with the hard X-ray tail extending at least to 220 keV. The spectral parameters derived for those observations are shown in Table 2. Similarly, we defined a strong non-detection when 1) the SNR in the 75–220 keV is < 1 , and 2) the F-Test was at a level of $\gtrsim 10^{-5}$. We thus observed (see Table 1) 4 strong non-detections. We note that several of our observations have very significant F-Test values, but with an SNR < 5 . In those cases we do not claim that we have observed a hard X-ray tail, although this is an open possibility. In Figure 1 we show one of our clear detection spectra, together with a spectrum when we have not detected a hard component.

We observed a variation of a factor of ~ 3 in the flux of the non-thermal component in the 20–200 keV

Table 1. Selected RXTE Data Observations of Sco X-1

OBSID	MJD	No.	Z Pos.	Live Time ^a	SNR ^b	F ^c	Flux ^d	Hard Tail	(Y/N)
20053-01-01-00	50556	1	HB	6341	10.6	4.4E-15	$8.57^{+1.52}_{-1.38}$		Y
20053-01-01-02	50558	2	NB	5434	4.2	1.7E-7	$4.05^{+0.57}_{-0.87}$		
20053-01-01-03	50559	3	NB	5896	4.8	3.9E-9	$5.20^{+0.75}_{-0.74}$		
20053-01-01-05	50561	4	NB	1908	0.8	6.2E-5	$6.29^{+1.77}_{-1.77}$		N
20053-01-01-05	50561	5	FB	4593	2.4	7.7E-4	$2.47^{+1.94}_{-1.51}$		
20053-01-01-06	50562	6	NB	8558	7.3	3.5E-13	$8.63^{+0.91}_{-0.90}$		Y
10061-01-03-00	50815	7	NB	5484	4.2	2.7E-9	$5.48^{+0.69}_{-0.74}$		
20053-01-02-00	50816	8	FB	8145	18.6	5.8E-12	$13.6^{+2.0}_{-2.0}$		Y
20053-01-02-03	50819	9	NB	5686	3.5	2.7E-9	$5.91^{+0.96}_{-0.95}$		
30036-01-01-000	50820	10	FB	6858	5.8	3.8E-7	$7.73^{+1.62}_{-1.65}$		Y
20053-01-02-04	50820	11	FB	4193	4.9	3.3E-4	$3.44^{+1.23}_{-1.00}$		
30036-01-02-000	50821	12	NB	4370	2.2	3.6E-4	$4.50^{+0.87}_{-0.90}$		
30036-01-02-000	50821	13	FB	2527	1.8	3.6E-4	$2.83^{+1.05}_{-1.06}$		
30406-01-02-00	50872	14	NB	2326	2.5	1.0E-6	$4.03^{+1.07}_{-1.13}$		
30406-01-02-00	50872	15	FB	3125	< 0	0.08	< 2.20		N
30035-01-01-00	50963	16	HB	6253	6.2	1.2E-14	$3.63^{+0.92}_{-0.88}$		Y
30035-01-03-00	50965	17	NB	3750	1.3	2.4E-8	$3.20^{+0.86}_{-0.89}$		
30035-01-03-00	50965	18	FB	2318	< 0	0.03	< 2.67		N
30035-01-04-00	50966	19	FB	6230	< 0	0.38	< 1.00		N
40020-01-01-00	51186	20	NB	2669	6.6	1.2E-7	$6.10^{+2.21}_{-2.10}$		Y
40020-01-01-01	51186	21	NB	4233	3.5	3.3E-8	$3.77^{+1.66}_{-1.45}$		
40020-01-01-02	51187	22	FB	8000	8.1	2.2E-9	$7.40^{+2.46}_{-0.94}$		Y
40020-01-01-04	51188	23	NB	2836	1.8	1.1E-3	$3.00^{+1.28}_{-1.20}$		
40020-01-01-04	51188	24	FB	1822	1.8	0.11	$2.95^{+2.12}_{-2.48}$		
40020-01-01-05	51189	25	SA	4316	2.9	5.6E-4	$2.57^{+0.88}_{-0.87}$		
40020-01-03-00	51193	26	HB	3578	6.2	9.8E-10	$8.45^{+1.94}_{-1.69}$		Y
40706-01-01-000	51433	27	NB	8076	2.8	1.4E-5	$2.09^{+0.55}_{-0.53}$		
40706-01-01-000	51433	28	FB	2167	2.2	1.2E-3	$2.45^{+1.04}_{-1.07}$		

Note: HB=Horizontal Branch, NB=Normal Branch, FB=Flaring Branch;
 SA=Soft Apex ; No.=observation number

^a total live time for HEXTE, in s

^b signal to noise ratio in the 75-220 keV energy range

^c probability that a better fit occurred due to a random chance

^d flux in the 75–220 keV energy range, in units of 10^{-10} ergs cm $^{-2}$ s $^{-1}$; apart from the 5 detections of a hard X-ray tail, the photon index used for the non-thermal component was our average value of ~ 1 ; uncertainties are given at 90 % confidence level

Table 2. Hard X-ray Tail Detections in Sco X-1

OBSID	No.	Bremsstrahlung		Power-Law		χ^2_ν	Z Pos.
		kT (keV)	Flux ^a	Γ	Flux ^b		
20053-01-01-00	1	$4.83^{+0.04}_{-0.05}$	$9.03^{+0.39}_{-0.36}$	$1.75^{+0.22}_{-0.20}$	$1.56^{+0.10}_{-0.11}$	1.59	HB
20053-01-01-06	6	$4.50^{+0.05}_{-0.05}$	$5.83^{+0.30}_{-0.27}$	$1.64^{+0.29}_{-0.27}$	$0.91^{+0.11}_{-0.10}$	1.06	NB
20053-01-02-00	8	$4.36^{+0.03}_{-0.03}$	$7.16^{+0.26}_{-0.24}$	$-0.17^{+0.30}_{-0.33}$	$1.22^{+0.13}_{-0.14}$	1.26	FB
30036-01-01-000	10	$4.28^{+0.03}_{-0.04}$	$9.63^{+0.42}_{-0.41}$	$-0.71^{+0.63}_{-0.70}$	$0.63^{+0.11}_{-0.11}$	1.29	FB
30035-01-01-00	16	$4.51^{+0.08}_{-0.07}$	$7.45^{+0.60}_{-0.67}$	$2.37^{+0.33}_{-0.28}$	$1.04^{+0.08}_{-0.08}$	1.09	HB
40020-01-01-00	20	$4.54^{+0.06}_{-0.07}$	$4.07^{+0.24}_{-0.20}$	$1.00^{+0.53}_{-0.49}$	$0.75^{+0.16}_{-0.15}$	1.13	NB
40020-01-01-02	22	$4.41^{+0.02}_{-0.02}$	$7.46^{+0.15}_{-0.15}$	$-0.49^{+0.42}_{-0.24}$	$0.66^{+0.12}_{-0.12}$	1.67	FB
40020-01-03-00	26	$4.69^{+0.04}_{-0.05}$	$6.20^{+0.25}_{-0.25}$	$1.36^{+0.26}_{-0.27}$	$1.24^{+0.13}_{-0.15}$	1.80	HB

Note: bremsstrahlung + power law model used;

uncertainties are given at 90 % confidence level for the derived parameters of the model applied

^a Flux in 20–50 keV range in units of 10^{-9} ergs cm $^{-2}$ s $^{-1}$

^b Flux in 20–200 keV interval in units of 10^{-9} ergs cm $^{-2}$ s $^{-1}$

interval among our 8 detections, and, at least, an order of magnitude in overall variability, taking into account our entire database.

We were also able to study the time-scale of variations of the hard X-ray component. As can be seen in Table 1, for observation 20 we detected a hard X-ray tail, which was not present 4 hours later in observation 21. To our knowledge, this is the first time that such a short time-scale variability in the hard component is reported for Sco X-1.

We also note that on all 3 occasions that the source was in the HB, a hard X-ray tail was detected.

DISCUSSION

Taking 2.5 kpc as the lower limit to the distance to Sco X-1 (Bradshaw, Fomalont, and Geldzahler, 1999), we found (using the PCA data) Sco X-1 to be emitting near the Eddington level in the 2–20 keV band (for a $1.4 M_\odot$ neutron star). This is remarkably different from the atoll sources (Barret et al., 2000), in which the luminosity in the same energy range is below 10^{37} ergs s $^{-1}$ when a hard tail is detected. The 20–200 keV hard component luminosity variation between our 8 detections is 5.9 – 15.0×10^{35} ergs s $^{-1}$, which is comparable to the weaker atoll sources hard X-ray luminosities reported by Barret, McClintock, and Grindlay (1996).

We have observed the presence of a hard X-ray tail in each of the 3 branches on the Z diagram. Although it is unclear what is producing the hard X-ray tail in Sco X-1, as can be seen in Figure 2a, it appears that the chance of observing a hard X-ray tail is greater if the thermal component is brighter. This assumes that the thermal component observed in HEXTE 20–50 keV band can be used to trace its $E < 20$ keV behavior. When we do observe a hard component, the power law index is correlated with the soft component temperature. (Figure 2b). One other interesting and suggestive relationship (Figure 2c) is that the hard component flattens as the mass accretion rate (\dot{M}) increases, if we assume that the movement along the Z diagram (from the horizontal to the flaring branch) is the result of the increasing variation of the \dot{M} (see, e.g., van der Klis, 1995). Thus it is possible to speculate that the mechanism responsible for the production of the hard component and its shape is dependent on the \dot{M} , the 20–50 keV flux, and temperature of the soft thermal component. We note that while is straightforward to explain the derived power law indices, and the hard X-ray emission, when the source was observed in the HB and in the FB in terms of synchrotron emission or Comptonization models, our measured photon indices in the FB (consistent with 0) are not compatible with the hard X-ray emission being produced by one of those two mechanisms.

Our HEXTE observations 20–22 and 26 (see Table 1) overlap with BATSE/OSSE observations reported in Strickman and Barret (2000). It is interesting to note that while HEXTE detected the presence of the hard X-ray tail in observations 20 and 22, BATSE/OSSE did not. Meanwhile, in observation 26 the hard X-ray tail was detected both by HEXTE and BATSE/OSSE, with a spectrum extending up to ~ 400 keV.

Our measured luminosities in the 2–20 keV (L_x) and 20–200 keV energy intervals (L_{hx}) can be used

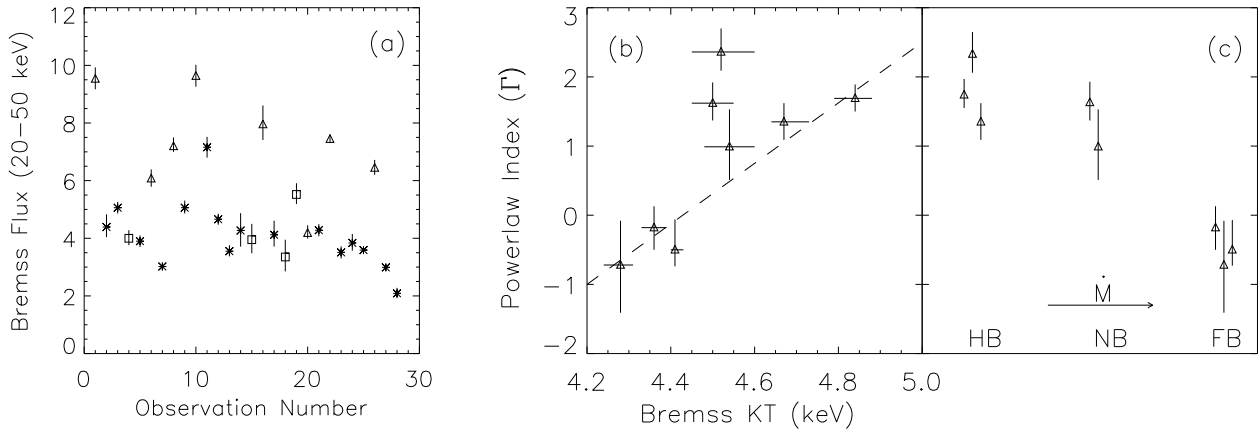


Fig. 2. a) The thermal flux as measured by HEXTE (in units of 10^{-9} ergs cm^{-2} s^{-1}) for our entire database, which suggests that the chance of observing a hard X-ray tail (triangles) is higher when the thermal component is brighter. Squares are strong non-detections of a hard component (see Table 1) and asterisks are treated as intermediate cases (see text). b) When a hard tail is observed, there is also some tendency for it to be steeper as the temperature of the thermal component increases. c) Plotting the power-law observed against the branch in the Z suggests that a higher \dot{M} makes the hard X-ray spectrum flatter (see text for details). In (c), HB, NB and FB were arbitrarily spaced along the x axis.

to study the suggestion (Barret et al., 2000) that such luminosities can be used to distinguish between neutron star and black hole systems, with neutron stars systems emitting $L_{hx} \sim L_x$ when $L_x \lesssim L_{crit}$, with $L_{crit} = 1.5 \times 10^{37}$ ergs s^{-1} . Since Sco X-1 is emitting close to the Eddington level, our observations can not be used to test the hypothesis for the 2–20 keV luminosity (see details in Barret et al., 2000). Otherwise our observations of L_{hx} are in agreement with the idea that only black hole binaries can have both L_x and L_{hx} above L_{crit} .

CONCLUSIONS

In this paper, we provided clear evidence for variable hard X-ray emission from the Z source Sco X-1. We observed that the 20–200 keV non-thermal component varied by at least an order of magnitude. We were able to track the movement of the source along the Z diagram and we concluded that the presence of the hard X-ray tail is not confined to a particular position in such a diagram, which may suggest that the mechanism responsible for the production of the hard X-ray tail is not uniquely dependent on the inferred \dot{M} . Otherwise we speculated that the appearance of a hard component in the spectrum may be related to the brightness of the thermal component, and that the shape of the X-ray tail may be correlated with the temperature of the thermal component.

ACKNOWLEDGMENTS

This research has made use of data obtained through the High Energy Astrophysics Science Archive Research Center Online Service, provided by the NASA/Goddard Space Flight Center. F. D'Amico gratefully acknowledges FAPESP/Brazil for financial support under grant 99/02352-2. This research was supported by NASA contract NAS5-30720.

REFERENCES

- Barret, D., and G. Vedrenne, Hard X-ray Emission from Weakly Magnetized Neutron Stars, *ApJS*, **92**, 505–510, 1994.
- Barret, D., J. E. McClintock, and J. E. Grindlay, Luminosity Differences Between Black Holes and Neutron Stars, *ApJ*, **473**, 963–973, 1996.
- Barret, D., J. F. Olive, L. Boirin, C. Done, G. K. Skinner, and J. E. Grindlay, Hard X-ray Emission from

Low Mass X-ray Binaries, *ApJ*, **533**, 329–351, 2000.

Bradshaw, C. F., E. B. Fomalont, and B. J. Geldzahler, High-Resolution Parallax Measurements of Scorpius X-1, *ApJ*, **512**, L21–L24, 1999

D’Amico, F., W. A. Heindl, R. E. Rothschild, and D. E. Gruber, HEXTE Detections of Hard X-ray Tails in Sco X-1, accepted by *ApJL* (astro-ph 0008279).

Di Salvo, T., L. Stella, N. R. Robba, M. van der Klis, L. Burderi, et al., The discovery of a State Dependent Hard Tail in the X-ray Spectrum of the Luminous Z-source GX 17+2, accepted by *A&A* (astro-ph 0009434).

Duldig, M. L., J. G. Greenhill, K. B. Fenton, R. M. Thomas, and D. J. Watts, Enhanced X-ray Emission Above 50 keV in Sco X-1, *ApSS*, **95**, 137–144, 1983.

Frontera, F., N. Masetti, M. Orlandini, L. Amati, E. Palazzi, et al., Discovery of Hard X-ray Emission from Type II Bursts of the Rapid Burster, to appear in X-ray Astronomy ’99 – Stellar Endpoints, AGN and the Diffuse Background, ed. G. Malaguti, G. G. C. Palumbo, and N. E. White (astro-ph 0007345).

Greenhill, J. G., M. J. Coe, S. J. Bell-Burnell, K. T. Strong, and G. F. Carpenter, High Energy X-ray Observations of Sco-like Sources with *Ariel V*, *MNRAS*, **189**, 563–570, 1979.

Haymes, R. C., F. R. Harnden, Jr., W. N. Johnson III, H. M. Prichard, and H. E. Bosh, The Low-Energy Gamma-ray Spectrum of Scorpius X-1, *ApJ*, **172**, L47–L49, 1972.

Heindl, W. A., and D. M. Smith, The X-ray Spectrum of SAX J1808.4–3658, *ApJ*, L35–L38, 1998.

Iaria, R., L. Burderi, T. Di Salvo, A. La Barbera, and N. R. Bobba, The composite Broad Band Spectrum of Cir x-1 at the Periastron: a Peculiar Z-source, accepted by *ApJ* (astro-ph 0009183).

Jahoda, K., J. H. Swank, A. B. Giles, M. J. Stark, T. Strohmayer, et al., In Orbit Performance and Calibration of the Rossi X-ray Timing Explorer (RXTE) Proportional Counter Array (PCA), *Proc. SPIE*, **2808**, 59–70, 1996.

Peterson, L. E., and A. S. Jacobson, The Spectrum of Scorpius XR-1 to 50 keV, *ApJ*, **145**, L962–L965, 1966.

Rothschild, R. E., D. E. Gruber, F. K. Knight, P. L. Nolan, Y. Soong, et al., A High Sensitivity Determination of the Hard X-ray Spectrum of Sco X-1, *Nature*, **286**, 786–788, 1980.

Rothschild, R. E., P. R. Blanco, D. E. Gruber, W. A. Heindl, D. R. MacDonald, et al., In-flight Performance of the High Energy X-ray Timing Experiment on the *Rossi X-ray Timing Explorer*, *ApJ*, **496**, 538–549, 1998.

Soong, Y., and R. E. Rothschild, Long-Term Hard X-ray Observations of Scorpius X-1 from *HEAO-1*, *ApJ*, **274**, 327–332, 1983

Strickman, M., and D. Barret, Detection of Multiple Hard X-ray Flares from Sco X-1 with OSSE, in Proceedings of the Fifth Compton Symposium, ed. M. L. McConnell, and J. M. Ryan, pp. 222–226, AIP, New York, NY, 2000.

van der Klis, M. in X-Ray Binaries, ed. W. H. G. Lewin, J. V. Paradijs, and E. P. J. van den Heuvel, pp. 252–307, Cambridge University Press, Cambridge, UK, 1995.